sustainability

MDPI

Article

Energy-Saving Potential of Building-Integrated Photovoltaic Technology Applied to a Library in Changsha, China

Genqiang Xian [1], Zhiyin Duan [1,*], Keqin Shan [1] and Xuelin Dong [2]

[1] Beijing Key Lab of Heating, Gas Supply, Ventilating and Air Conditioning Engineering, Beijing University of Civil Engineering and Architecture, Beijing 100044, China; 2108590022256@stu.bucea.edu.cn (G.X.); 2108590022212@stu.bucea.edu.cn (K.S.)
[2] Key Laboratory of Petroleum Engineering, China University of Petroleum, Beijing 102249, China; dongxl@cup.edu.cn
* Correspondence: duanzhiyin@bucea.edu.cn

Abstract: With the increasing number of public buildings worldwide, their energy consumption has garnered significant attention. This study aims to promote building energy efficiency and emission reduction by exploring the application of Building-Integrated Photovoltaic technology in library retrofitting. Using a library in Changsha City as a case study, we conducted an energy consumption analysis of the building's envelope and identified the window section as the highest energy consumer. We proposed a novel improvement scheme—the sun-shading photovoltaic panel (which shades the sun while generating electricity). Additionally, we utilized the roof space for the installation of conventional photovoltaic panels. Simultaneously, the primary objective of this paper was to derive a renovation strategy for public buildings in regions characterized by high summer temperatures and low winter temperatures based on the renovation case of this library. This paper comprehensively investigates the length and angle of sun-shading photovoltaic panels facing different directions, as well as the azimuth angle, tilt angle, and installation spacing of the conventional photovoltaic panels on the roof. Two retrofitting schemes were proposed. Through simulation and comparison, the second scheme was found to reduce the annual electricity consumption by 1,233,354 kWh, achieving a 35.4% decrease compared to the original building. Using the Changsha library as a template for public buildings, this study provided a retrofitting approach with Building-Integrated Photovoltaic technology via DesignBuilder, which could be extended to other geographic locations. The results demonstrated the significant energy-saving effects of the proposed retrofitting scheme.

Keywords: BIPV; optimal design; building energy simulation; energy saving; DesignBuilder

check for updates

Citation: Xian, G.; Duan, Z.; Shan, K.; Dong, X. Energy-Saving Potential of Building-Integrated Photovoltaic Technology Applied to a Library in Changsha, China. *Sustainability* **2024**, *16*, 9565. https://doi.org/10.3390/su16219565

Academic Editor: Gerardo Maria Mauro

Received: 31 July 2024
Revised: 21 October 2024
Accepted: 31 October 2024
Published: 2 November 2024

Copyright: © 2024 by the authors. Licensee MDPI, Basel, Switzerland. This article is an open access article distributed under the terms and conditions of the Creative Commons Attribution (CC BY) license (https://creativecommons.org/licenses/by/4.0/).

1. Introduction

With the rapid development of the global economy, energy crises and global warming have garnered increasing attention worldwide. Construction, transportation, and industry are collectively referred to as the "three energy giants" in China, with construction's energy consumption accounting for 32% of global energy consumption [1]. Carbon emissions from China's construction industry represent approximately 20% of the total emissions. In response to global climate change, China has pledged to peak carbon emissions by 2030 and achieve carbon neutrality by 2060. Therefore, reducing the use of fossil fuels and exploring renewable energy sources is an urgent priority.

As a nation rich in solar resources, China possesses a theoretical land solar energy-resource reserve of 17 trillion kilowatts, with regions receiving over 2000 h of annual sunshine accounting for two-thirds of the total area. Hunan province fell within this category of abundant-solar-resource regions, with annual solar radiation levels ranging approximately from 3780 to 5040 MJ/(m^2·a) [2]. This abundance provided favorable conditions for photovoltaic (PV) systems, which serve as a vital pathway towards achieving "zero carbon" emissions. Research by Alberto et al. [3] had demonstrated the significant potential of PV tech-

nology, showing that if every household in Mexico installs 3.59 PV panels, the country could save 39,750 GWh of electricity annually, representing 71% of national energy consumption. Similarly, studies by Ishii et al. [4] projected that by 2050, Japan could reduce annual greenhouse gas emissions from buildings from 1126 Gg CO_2-eqy^{-1} to 364.4b~410.4 Gg CO_2-eqy^{-1} through the installation of PV systems and cogeneration technologies. However, PV systems were heavily reliant on external conditions such as local solar radiation, outdoor temperature [5], wind speed [6], and PV module temperature. Therefore, the dynamic fluctuations in PV panels' efficiency due to changes in outdoor environmental parameters necessitated accurate prediction models to mitigate uncertainties and enhance system stability and grid quality.

Researchers employ extensive experimental simulations to predict the dynamic efficiency of PV panels, categorizing prediction models into two main types: direct and indirect prediction models. Direct prediction models utilize historical data, including meteorological parameters and PV electricity generation, to forecast PV panel output. Kaplanis et al. [7] investigated the impact of environmental temperature, wind speed, and solar radiation intensity on the photovoltaic panel power-generation prediction model, while Gulin et al. [8] also established and validated a prediction model for the power output of a photovoltaic array based on temperature and solar radiation intensity. In contrast, indirect prediction models first forecasted solar radiation at different times using various methods, such as numerical weather prediction (NWP), image-based methods, statistical approaches, and hybrid artificial neural networks (ANNs) [9–11]. Subsequently, these solar radiation parameters were input into commercial PV-simulation software like TRNSYSM, PVFORM, and HOMER for prediction. While both types of models contributed to this field of research, they emphasize different aspects. The research in this paper utilizes an indirect prediction model.

The integration of solar photovoltaic systems with buildings is known as Building-Integrated Photovoltaics (BIPVs). BIPV technology entails installing solar PV equipment on building surfaces, enabling the integration of electricity generation with building materials [12]. The principle of BIPV operation is similar to conventional PV electricity generation, wherein renewable solar energy is converted into electricity for building use. However, the key distinction lies in the ability of BIPV components to integrate with or serve as part of the building structure, thus reducing construction system costs [13]. Solar PV technology not only decreases conventional fossil fuel usage but also reduces carbon emissions and peak electricity demand. BIPVs primarily transforms energy-consuming buildings into energy-producing ones. This transformation involves the genuine integration of BIPVs with building products, such as roof sections, exterior walls, and windows. However, buildings' walls and roofs have limitations, especially considering the extensive use of glass curtain walls in modern architecture. Balancing energy provision and daylighting through Semitransparent Photovoltaic (STPV) glass is crucial, as increased energy generation from STPV glass may lead to decreased interior daylighting. Research by Johnson et al. [14] examined the impact of glass systems on the load and annual energy consumption of typical office buildings, indicating that effective daylight utilization significantly reduces lighting's energy consumption. They also identified a critical threshold for the window area beyond which cooling loads increase. Lee et al. [15] analyzed various window systems in five Asian climates and assessed their impact on buildings' energy consumption and visual daylighting through U-values, SHGC, and TV values under different climatic conditions. They found that U-values have a greater impact on heating loads than cooling loads, recommending low-U-value glass for heating-demanding regions. Presently, approximately 80% of BIPV products worldwide are installed on rooftops, with the remaining 20% installed on surfaces and windows [16]. The tilt angle and azimuth angle are two crucial factors affecting PV panel output. The tilt angle refers to the angle of PV modules relative to the horizontal plane [17], while the azimuth angle represents the angle of PV modules relative to true south, with −90° indicating due east, 0° due south, and +90° due west [18,19]. Some scholars have studied the tilt angle of PV panel installations. According

to the theoretical research by Hartner and Siraki [20,21], PV panel productivity is highest when the installation angle in southern regions of the Northern Hemisphere falls between θ and θ−15°. Benghanem et al. [22] developed a method using mathematical and statistical approaches to determine the optimal tilt angle for any location worldwide, concluding that the annual optimal tilt angle of solar panels approximated the local latitude. Regarding studies on the azimuth angle of PV panel installations, Mah et al. [23] determined the optimal azimuth angle for PV panel installations in the Huddersfield region of the UK through experiments and probabilistic modeling. Additionally, for building window sections, He et al. [24] compared the performance of single-layer and double-layer STPV glass through simulation, finding that double-layer STPV glass had greater potential for energy saving and emission reduction. Young et al. [25] conducted experimental tests on two identical buildings—one installed with BIPV glass and the other with ordinary single-layer tempered glass. By simulating and analyzing with CFDesign and Ecotect software, they concluded that the building with BIPV glass experienced approximately 27.3% lower annual energy consumption than the one with single-layer tempered glass.

Most current studies focus on retrofitting individual modules of buildings, such as roofs, windows, or exterior surfaces, employing relatively singular technologies. Singh [26] proposed a method to estimate the solar energy potential of roofs in a specific area by simulating and estimating the PV roof area using PVSyst combined with ASHRAE manual environmental parameters and using the Liu–Jordan model to estimate solar radiation on PV arrays. Zhong [27] utilized the Maximum PV Panel Coverage-Rate Algorithm (MPPCP) combined with Geographic Information Systems (GISs) to divide roof areas into regular grids using a discretization method, evaluating grid units to optimize the installation of multiple PV panels in different scenarios. However, research on multi-technology coupled multi-module transformations was limited. We chose the library as the target building mainly because it is a representative public building with an average daily operation time of about 15 h. Additionally, the building has a high window-to-wall ratio, close to 0.5, which leads to higher energy consumption, making energy-saving renovations particularly important. This paper carries out multi-module coupled energy-saving renovations on the library by utilizing technologies such as PVs, BIPVs, and external shading. Through simulation using DesignBuilder software, the optimal retrofitting scheme was determined. Specific retrofitting structures included installing PV panels on the roof, replacing windows with BIPV structures and external shading, and installing PV panels on external shading [25].

Despite the increasing attention on Building-Integrated Photovoltaics (BIPVs) in recent years, most existing studies primarily focus on individual building components, such as roofs or walls, while overlooking the combined effects of multiple building modules and technologies. Additionally, limited research has explored the application of BIPV technology specifically in regions with hot summers and cold winters, such as Changsha. This study addresses these gaps by integrating BIPVs with horizontal sunshades and roof-mounted PV panels to evaluate the energy-saving potential in a comprehensive retrofitting approach. Our contribution lies in developing a validated simulation model using DesignBuilder to optimize tilt angles, azimuth angles, and shading structures for BIPV systems in this specific climate condition. By comparing simulation results with experimental data, this study not only proposes an effective retrofit solution for the target library but also provides a transferable methodology applicable to other public buildings in similar climates. Due to the retrofitting methods presented in this paper, which result in a reduction of solar heat-gain during the winter (which is beneficial), the application is only suitable for regions with milder winters. In such areas, the buildings require less solar heat-gain during the winter, leading to a minimal increase in heating energy consumption. Otherwise, even if the cooling energy consumption is reduced by decreasing summer solar heat-gain, the heating energy consumption during the winter would significantly increase.

2. Research Methods

2.1. Modeling Method

This study evaluates the performance of Building-Integrated Photovoltaic (BIPV) technology in the hot-summer and cold-winter climate of Changsha by combining qualitative and quantitative analysis. A comprehensive building-energy-performance model was developed using a combination of experimental testing and numerical simulation. In the experimental phase, meteorological data were collected, and the building's energy consumption was monitored. In the simulation phase, the DesignBuilder software(V7) was used to optimize key parameters such as the tilt angle, azimuth angle, and shading structure of the photovoltaic panels. Subsequently, the BIPV system was applied in different configurations, including rooftop solar panels, photovoltaic windows, and external shading devices. The following diagram illustrates the overall research process, with explanations provided for each section (Figure 1).

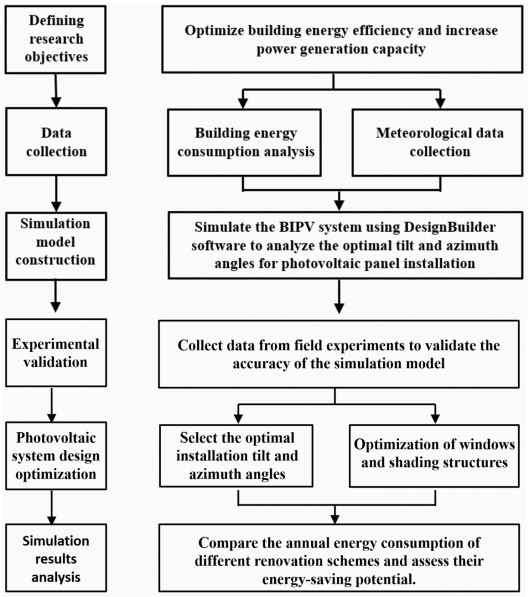


Figure 1. Diagram of the research methodology.

2.1.1. Geometry of Model

The building is situated in Changsha, Hunan Province, with a climate characterized by hot summers and cold winters. The library features six above-ground floors with a total height of 27 m (Figure 2). The total above-ground floor area is approximately 25,001.57 m^2, and the total above-ground volume is approximately 126,178.51 m^3. The overall orientation of the building is northward at 83.40°, with a form factor of 0.13. Levels one through four feature atrium structures, while levels five and six consist of top-floor voids.

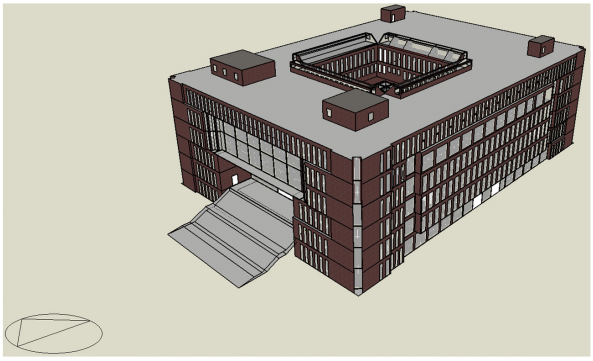


Figure 2. 3-D model of the library.

2.1.2. Thermophysical Parameters of Building Envelope

Exterior Wall

The library's exterior wall is composed of multiple layers with a total thickness of approximately 290 mm. From the innermost layer to the outermost layer, it consists of the following materials: a 10 mm thick brick layer, a 30 mm thick FOAMGLAS insulation board, a 20 mm thick cement mortar layer, a 200 mm thick autoclaved aerated concrete block, another 20 mm thick cement mortar layer, and, finally, a 10 mm thick finishing mortar and coating layer. Specific thermophysical parameters of the wall materials are provided in Table 1.

Table 1. Thermophysical parameters of the external wall materials for the library.

Wall Materials					
Layers	**Thickness**	**Density**	**Thermal Conductivity**	**Thermal Capacity**	**U-Value**
	mm	**kg/m^3**	**W/(m·k)**	**kJ/(kg·K)**	**W/(m^2·K)**
Block paving	10	1900	1	1.05	1.191
FOAMGLAS insulation board	30	140	0.062	0.84	
Cement mortar	20	1800	0.93	0.837	
Autoclaved aerated concrete block	200	566	1.8	1.047	
Decorative mortar	10	1800	0.93	0.837	

Roof

The library building's roof features an energy-efficient technology known as a green roof. Green roofs are a type of passive energy-saving technique, and a detailed explanation of green roofs will be provided in the third section. The roof structure is also composed of multiple layers, from the topmost layer to the internal part of the roof, as follows: a 300 mm thick planting soil layer, a 40 mm thick fine aggregate concrete layer, a 6 mm thick waterproofing layer, a 20 mm thick cement-mortar leveling layer, a 100 mm thick extruded polystyrene board, a 120 mm thick reinforced-concrete roof slab, and a 20 mm thick mixed mortar layer. Specific parameters of the roof materials are provided in Table 2.

Table 2. Thermophysical parameters of the roof materials for the library.

Roofing Materials					
Layers	**Thickness**	**Density**	**Thermal Conductivity**	**Thermal Capacity**	**U-Value**
	mm	**kg/m^3**	**W/(m·K)**	**kJ/(kg·K)**	**W/(m^2·K)**
ECO roof material	300	1000	0.3	1	0.215
Fine aggregate concrete	40	2321	1.74	0.754	
PVC	6	1390	0.17	0.9	
Cement mortar	20	1800	0.93	0.837	
Extruded polystyrene board	100	40	0.03	2.47	
Reinforced concrete	120	2500	1.74	0.837	
Mixed mortar	20	1700	0.87	0.837	

External Window

The windows and transparent curtain wall of the library have a relatively simple double-layer low-emissivity (low-e) glass structure consisting of 6 mm glass, a 12 mm air gap, and another 6 mm glass. The Solar Heat Gain Coefficient (SHGC) is 0.5, the visible transmittance is 0.6, and the glass thermal conductivity is 2.6. The building does not currently provide any shading design. However, in most buildings, the largest contributors to energy consumption are the Heating, Ventilation, and Air Conditioning (HVAC) systems and artificial lighting. Building shading is a passive energy-saving technology that not only

enhances the aesthetics of the building but also reduces its energy consumption. This is because solar radiation is a significant source of building heat-gain. The parameters of the glass structure in the library are listed in Table 3.

Table 3. Specific parameters of photovoltaic glass and original window glazing used in model.

Glass Material	Thickness (mm)	SHGC	VT	U-Value W/(m^2·K)
STPV glass (Glass 3 mm + Air 13 mm + Generic low-iron glass 3 mm)	3 mm + 13 mm + 3 mm	0.829	0.839	2.716
Double low-e glass (Glass 6 mm + Air 12 mm + Glass 6 mm)	6 mm + 12 mm + 6 mm	0.5	0.6	2.6

2.2. Experimental Method

The basis for this conclusion is drawn from the findings of reference papers [20] and [21]. The conclusions of these reference papers indicate that the optimal tilt angle range for photovoltaic panels in the Northern Hemisphere is from the latitude of the building (θ) to the latitude of the building minus 15 degrees (θ–15). Given that the latitude of the Changsha area is 28.22° (θ), it is concluded that the optimal tilt angle range for photovoltaic panels in the Changsha area is 13–28°. As the authors are located in Beijing, experimental verification of the simulation conclusions was conducted in Beijing, which is situated at a latitude of 39.54° N and longitude of 116.25° E. According to the theories of Har and Sir, the optimal tilt angle for annual electricity generation in Beijing is between 25–40°.

This study seeks to explore the effects of tilt and azimuth angles on PV panels' power output, identify the optimal angles for maximum generation, and analyze outdoor meteorological data to assess their influence on PV electricity production.

2.2.1. Experimental Testing System

Outdoor Environmental Parameter Measurement

(1) Weather Station

Outdoor environmental data in this experiment are obtained using a portable weather station. This device allows real-time observation and recording of air temperature, humidity, atmospheric pressure, wind speed, wind direction, Beaufort scale, rainfall, horizontal radiation, and total solar radiation. The data are stored in the cloud for later retrieval.

(2) Pyranometer

Solar radiation is measured using a pyranometer based on the thermoelectric method. The measurement range for solar radiation is 0 to 2000 W/m^2, with an accuracy of ±2% and a resolution of 1 W/m^2 (Figure 3, Table 4).

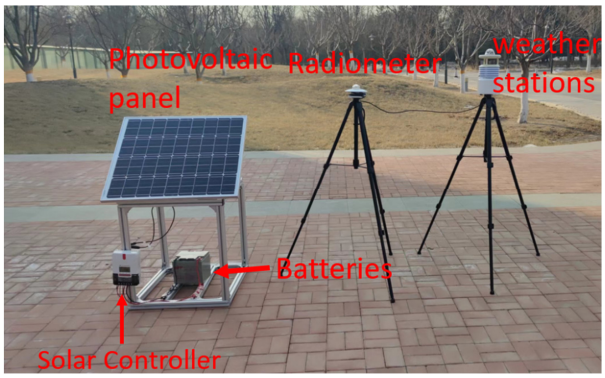


Figure 3. Weather station and thermopile radiometer.

Table 4. Specific parameters of weather stations and radiometers.

Portable weather station	JD-BQX	Air temperature	−40~100 °C	±0.3 °C (25 °C)	0.01 °C
		Air humidity	0~100% RH	±3% RH (60%RH, 25 °C)	0.01% RH
		Atmospheric pressure	300~1100 hpa	±0.25%	0.1 hpa
		Wind speed	0~70 m/s	±0.1 m/s	0.01 m/s
		Wind direction	0~360°	±1°	1°
		Hyetal	0~4 mm/min	±4%	0.1 mm
		Total solar radiation	0~2000 W/m^2	±5%	1 W/m^2
Thermopile solar radiation recorder	JD-BQX	Thermoelectric radiation	0~2000 W/m^2	±5%	1 W/m^2
		Spectral range		0.3~3 μm	

Outdoor Electricity-Generation Measurement

An outdoor photovoltaic power-generation system is assembled using PV panels (Singfosalar, China), a battery (12 V, 38 Ah), and a solar charge controller. The tilt angle of the PV panel is adjusted using an adjustable bracket to measure the electricity generation at different tilt angles. The electricity-generation data are obtained using the JIRI MPPT (JIRI, China) solar energy controller's backend software (Table 5).

Table 5. Parameters of PV panels.

Photovoltaic panel	SFM-100	Number of cells	36 (12 × 3)
		Overall dimension	770 mm * 671 * mm 25 mm
		Peak power	100 W
		Peak voltage	18 V
		Open-circuit voltage	21.6 V
		Peak current	5.56 A
		Short-circuit current	6.11 A
		Conversion efficiency	18–19%

2.2.2. Experimental Testing Plan

(1) Set the orientation angle to 0° (as per simulation results), and use a bracket to adjust the tilt angle of the photovoltaic panel. Tests of different tilt angles must be conducted under the same meteorological conditions.
(2) Place the weather station and radiometer next to the PV panel to test the outdoor meteorological parameters for the day, including dry-bulb temperature, relative humidity, total radiation, and wind speed. The daily PV panel electricity generation can be directly read from the controller.
(3) During the night, use a fan and thermal patches to consume the electricity generated during the day to prevent affecting the charging of the battery the next day.
(4) Process the data obtained from the weather station, import the processed data into DesignBuilder, and conduct simulations to obtain the simulated electricity generation for that day.

2.3. PV Panel Solar Radiation Calculation Methods

Total solar radiation includes direct radiation and diffuse radiation, where diffuse radiation consists of scattering through media such as clouds and scattering after direct radiation reaches surfaces like the ground. The direct radiation received by PV panels with tilt angles ($S_{incident}$) can be divided into the direct-radiation vertical component (S_{module}) and the direct-radiation horizontal component ($S_{module.h}$). The total radiation received on the surface of the PV panel (TPP) equals the direct-radiation vertical component (S_{module}) plus the diffuse radiation ($S_{diffuse}$). Among them, the horizontal component of direct radiation is parallel to the PV panel and cannot generate electricity, so only the vertical component of direct radiation affects the PV panel.

$$S_{incident} = S_{module} + S_{module.h} \quad (1)$$

where $S_{incident}$ is the amount of direct radiation received by the photovoltaic panel. S_{module} is the vertical component of the direct radiation. $S_{module.h}$ is the horizontal component of the direct radiation.

$$TPP = S_{module} + S_{diffuse} \tag{2}$$

where TTP is the total radiation received by the photovoltaic pane, W/m^2. $S_{diffuse}$ is the amount of diffuse radiation.

$$S_{incident} = \frac{S_{horizental}}{\sin \alpha} \tag{3}$$

where α is the complement of the solar elevation angle. $S_{horizontal}$ is the vertical component of the solar radiation to the ground.

According to Figure 4, it can be obtained that

$$S_{module} = S_{incident} \cdot \sin(\alpha + \beta) = \frac{S_{horizental}}{\sin \alpha} \cdot \sin(\alpha + \beta) \tag{4}$$

where β is the PV panel's tilt angle.

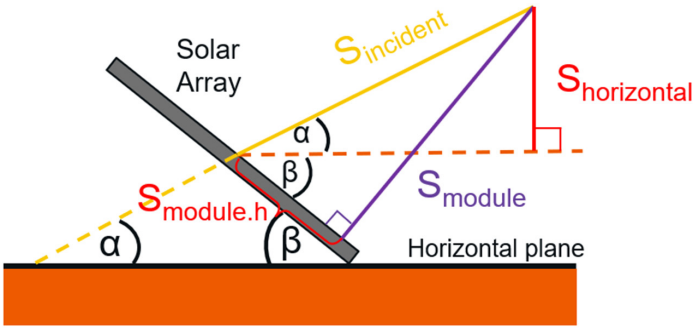


Figure 4. Schematic diagram of radiation reception by PV panel.

Therefore, the total radiation received by the PV panel is as follows:

$$TPP = S_{module} + S_{diffuse} = \frac{S_{horizental}}{\sin \alpha} \cdot \sin(\alpha + \beta) + S_{diffuse} \tag{5}$$

3. Model Validation

To validate the effectiveness and accuracy of the photovoltaic power generation model simulation, we conducted experimental verification. Figure 5 shows the outdoor meteorological parameters, and Figure 6 presents the experimental and simulation results. Experimental tests with different photovoltaic panel tilt angles were conducted during a period when outdoor meteorological parameters changed very little. From Figure 5, we can see that the power generation at 34° is the highest among all angles, and the simulation results also show that 34° yields the highest power generation. This consistency between experimental and simulation results demonstrates the reliability of the simulation method. Therefore, using this method to simulate the optimal tilt angle for the Changsha region is also credible. The differences between the experimental and simulation values may be due to the fact that the outdoor meteorological parameters used in the experiments are averaged over 30 min intervals, while in reality, these parameters (such as radiation and wind speed) fluctuate continuously during that period. However, in the simulation, the parameters remain constant.

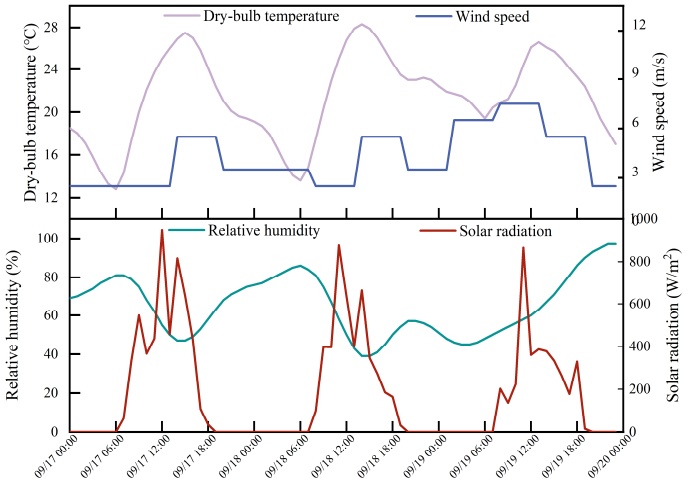


Figure 5. Outdoor weather data.

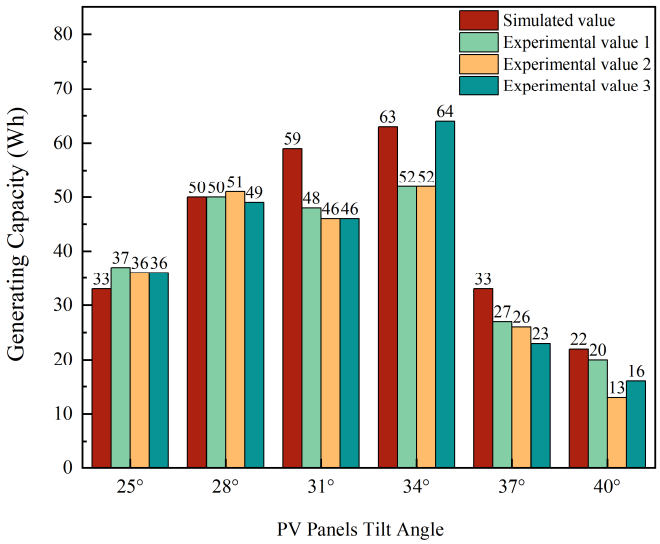


Figure 6. Experimental and simulated electricity generation of PV panels at different tilt angles.

4. Optimizations and Analyses

4.1. Predictions of Building Load

Due to the large window-to-wall ratio of the library building, the window-to-wall ratios for all four orientations range between 0.4 and 0.47. With window area comprising nearly half of the total facade area, energy consumption associated with windows requires particular attention. Through simulations, we compared the summer cooling load and winter heating load of the entire building, as depicted in Figure 7. From Figure 7, it is evident that the heating and cooling loads created by external windows constitute a significant portion of the overall building load, accounting for 55.6% in winter and 66.1% in summer. Therefore, reducing heat gain through the external windows in summer and decreasing heat loss from windows in winter are crucial for energy conversation due to their substantial contribution to the building's load.

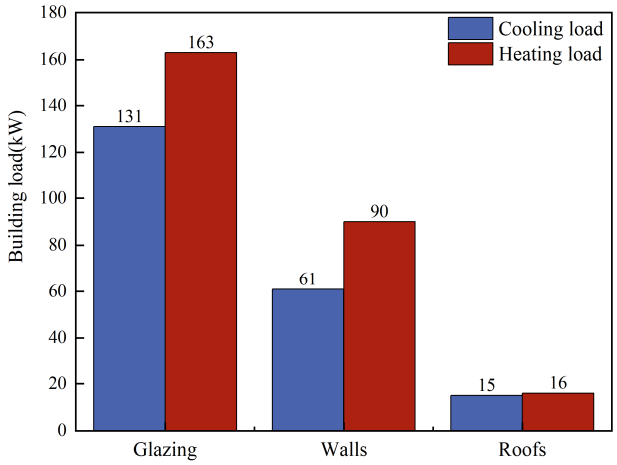


Figure 7. Modeling prediction of whole-building cooling and heating loads.

4.2. Optimization of PV Panel Installed on Roof Surface

The Tilt Angle and Azimuth Angle for Flat PV Panel Installation

The roof section, in comparison to the wall and window sections, offers more convenient conditions, such as longer sunlight exposure and lack of obstruction. Installing PV panels on the roof presents a simpler and more convenient solution compared to modifying glass and walls (Figure 8). The primary consideration when installing PV panels on the roof is the angle of inclination. With the building's latitude at 28°, the installation angle for PV panels ranges between 13° and 28°. It is necessary to select an angle within this range that maximizes annual yield. Therefore, we divided this range into five groups with intervals of 3° for comparison using a simplified model. Since the simplified model differs from the original only in size but shares the same roof installation, it effectively substitutes the original model without other influencing factors. The specific comparative results of these angles are shown in Figure 9. From this, it is evident that the highest productivity is achieved when the installation angle of the PV panels is 25°. Therefore, the PV panel installation angle on the library model's roof is set to 25° to achieve optimal annual yield.

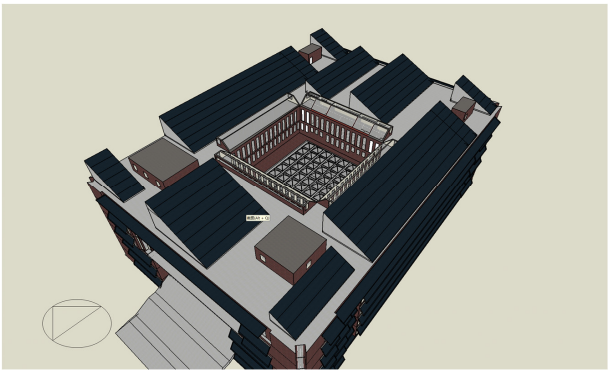


Figure 8. 3D model of PV panel.

Furthermore, different azimuth angles of the PV panels on the roof will also result in differences in system productivity. We utilized a simplified model to simulate the specific productivity of PV panels at different azimuth angles in the Changsha area, as depicted in Figure 10. Simulations were conducted at 15-degree intervals from due west to due east. The results indicate that panels facing due south exhibit the highest productivity. Therefore, the orientation of the PV panels on the library's roof is set to due south.

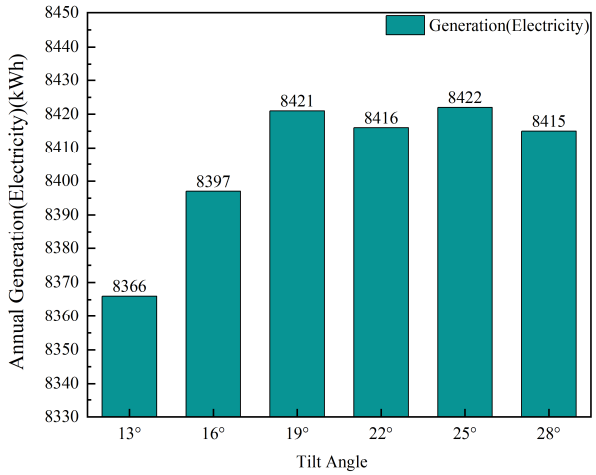


Figure 9. A graph showing electricity generation of rooftop PV panels for various tilt angles of PV panels.

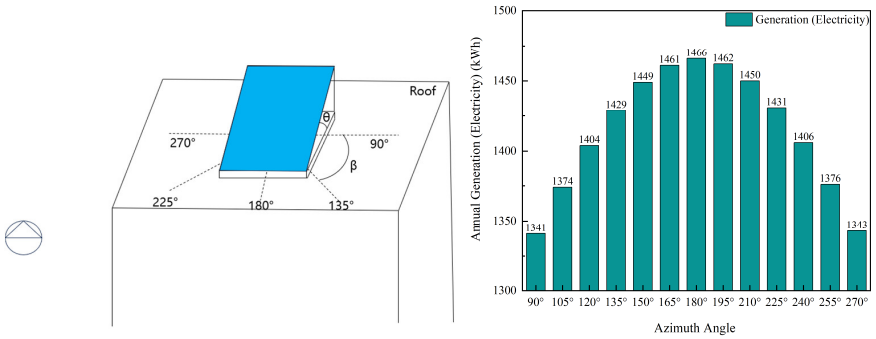


Figure 10. A graph showing electricity generation of rooftop PV panels for different azimuth angles.

4.3. Optimization of Window and Shading

4.3.1. Sun Path Variations Throughout a Year

Through an analysis of the solar paths at 09:00, 12:00, and 15:00 during the summer solstice, winter solstice, vernal equinox, and autumnal equinox in Changsha City, as illustrated in Figure 11, it is observed that throughout the year, the building facades predominantly receive sunlight from the east, west, and south directions. This suggests that the building facades facing these directions have the highest solar energy potential. Moreover, it is possible to determine which facades of the building can receive higher solar radiation at which times based on the building's shadow. For example, at 9 o'clock in the morning, the building's shadow indicates that there is little difference in solar radiation received by the south and east facades of the building in spring and autumn. However, in summer, the east facade receives more solar radiation than the south facade, and in winter, the south facade receives more solar radiation than the east facade. Additionally, based on our simulations, we have obtained comparative graphs of glass loads for the four orientations and solar radiation through the glass for the four orientations, as depicted in Figure 12. In winter, daylight hours are shorter, typically from 7:00 to 17:00, while in summer, daylight hours are longer, usually from 6:00 to 18:00. Only in June and July, around noon, do the sunlight rays nearly parallel the south-facing glass, making this period less favorable for south-facing photovoltaic glass. For the rest of the year, sunlight predominantly radiates onto the south-facing glass.

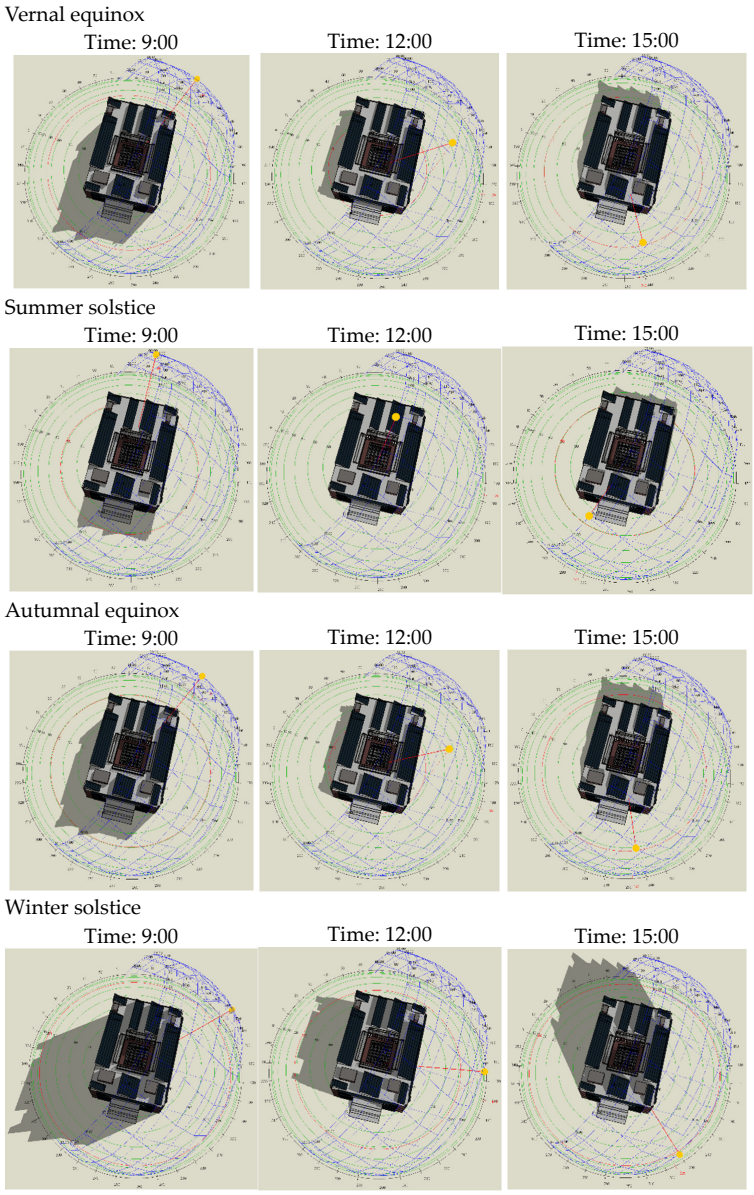


Figure 11. Photos of solar paths simulated by DesignBuilder.

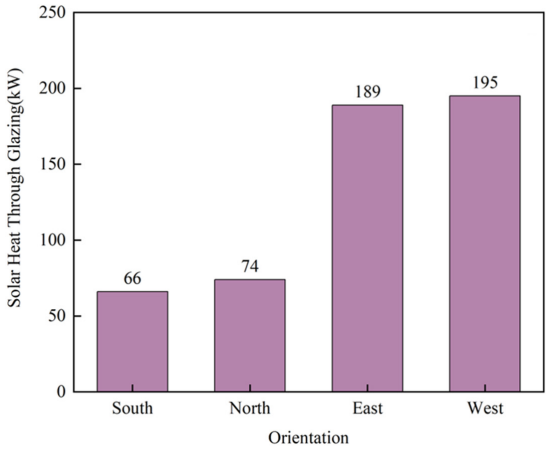


Figure 12. Comparison of solar radiation through glass with different orientations on 15 June 2002 (typical year).

4.3.2. Semitransparent Photovoltaic Glass

Semitransparent Photovoltaic Glass (STPV) is an energy-saving technology that integrates photovoltaic power generation on building surfaces, and it has garnered widespread attention in the architectural field in recent years. STPV windows not only allow partial transmission of natural light, improving indoor lighting conditions, but also utilize solar energy for power generation, reducing building energy consumption. As a result, STPV windows are considered multifunctional building components that combine thermal comfort, daylighting performance, and energy production.

The thermophysical properties of STPV glass are crucial for its energy-saving effectiveness in building applications. Its thermal conductivity, Solar Heat Gain Coefficient (SHGC), and Visible Transmittance (VT) directly influence the thermal environment and energy performance of buildings. In tropical and arid climates, STPV windows effectively reduce the cooling load of buildings by minimizing the amount of solar radiation entering indoors. For instance, Mesloub et al. [28] combined simulation and experimental methods to study the application of STPV windows in semi-arid climates of Algeria. The results showed that STPV windows not only significantly reduce building energy consumption but also achieve a balance between daylighting and shading by optimizing the window-to-wall ratio (WWR) and adjusting the transparency of the photovoltaic modules. Furthermore, another experimental study on office buildings in Algeria by Mesloub et al. [29] used detailed simulation methods to analyze the performance of STPV windows under different light transmittance and orientations. The study concluded that a well-designed STPV system can significantly improve a building's energy performance, particularly in terms of daylighting and thermal comfort. Moreover, the thermal transfer performance of STPV windows is influenced by material and structural design. Fund and Yang [30] found through simulation that the coverage area of solar cells within the photovoltaic modules is directly related to heat gain. When the solar cell coverage reached 80%, the total indoor heat gain was reduced by 70%. Therefore, a well-designed STPV window can not only reduce indoor heat load but also achieve a dynamic balance between daylighting and shading.

In terms of modeling techniques, recent numerical simulation studies have enabled precise evaluation of the energy performance of STPV windows under various climatic conditions. Mesloub et al. [31] employed a combination of experimental methods and simulation tools, including EnergyPlus and DIVA-for-Rhino, to compare different configurations of the PVSD (Photovoltaic Shading Device) and STPVs. The results demonstrated that at an optimal tilt angle of 30°, the unfilled eggcrate PVSD performed the best, with a photovoltaic conversion efficiency of up to 20%. This configuration significantly reduced air conditioning energy consumption while maintaining indoor visual comfort. Additionally, the integration of Internal Light Shelves (ILS) further improved indoor daylight uniformity and reduced glare issues caused by excessive daylighting. Mesloub et al. [32] conducted simulations to analyze various ILS configurations with different heights, reflective surface angles, and integrated photovoltaics with different coverage rates. The study identified an optimal arrangement that reduced energy consumption by 85%, eliminated glare, and provided uniform illumination.

In this study, the STPV window glass consists of 3 mm thick ordinary glass and a 13 mm air layer, offering high transparency and low thermal conductivity. Its SHGC is 0.829, VT is 0.839, and thermal conductivity is 2.716 $W/m^2 \cdot K$ (Table 3). Compared to traditional double-layer low-E glass, STPV windows exhibit significant advantages in both energy efficiency and daylight performance. Based on existing research, STPV windows can significantly reduce building energy consumption and improve indoor environmental comfort through proper design and parameter optimization. At the same time, Mesloub et al. [33] simulated the integration of ILS with STPV systems under various climatic conditions in different regions of the world. The results showed that the energy-saving rate exceeded 65% in all regions, and the combination effectively reduced discomfort caused by glare.

This modeling utilized an equivalent one-diode circuit model implemented in DesignBuilder to predict current-voltage characteristics of the photovoltaic modules. This model requires as inputs the open-circuit voltage, short-circuit current, current and voltage at the maximum power point, as well as the temperature coefficients for the short-circuit current and open-circuit voltage under reference conditions. These parameters can be obtained from manufacturers' technical specifications. The PV performance under operating conditions is determined by the one-diode model using the "four parameters", including the diode reverse-saturation current, the series resistance, the shunt resistance, and the curve-fitting parameter found in manufacturers' specifications.

4.3.3. External Shading with PV Panels

External shading is another method to reduce solar radiation, which directly blocks the sunlight from entering indoors, as shown in Figure 13. However, this method does not fully utilize the blocked solar radiation. Therefore, we applied PV panels on the outside surface of external shading to increase power generation. PV panel parameters are shown in Table 6. By installing PV panels on the external shading, it not only blocked solar radiation from entering indoors but also converted the blocked solar radiation into electricity to supply energy needs for buildings.



Figure 13. Cases for applying BIPV technologies (skylight and facade) to buildings [34,35].

Table 6. Specifications of the SINGFO-600 model photovoltaic panel.

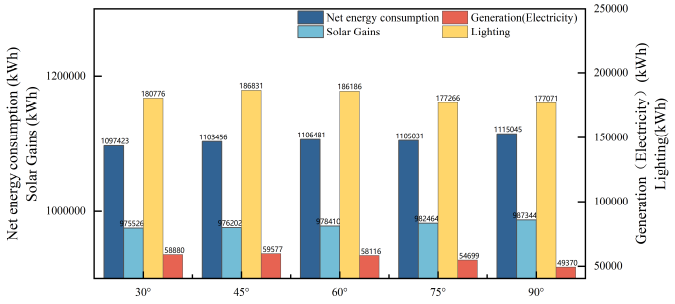
Parameters	Values	Parameters	Values
Maximum power (Pmax)	600 W	Temperature coefficient of open-circuit voltage (V/K)	−0.276%/°C
Open-circuit voltage (Voc)	49.55 V	Temperature coefficient of short-circuit current (A/K)	0.046%/°C
Short-circuit current (Isc)	15.43 A	Module efficiency (%)	20.00%
Optimum current (Imp)	14.42 A	NOCT insolation (W/m^2)	1000 W/m^2
Optimum voltage (Vmp)	41.62 V	Environmental temperature(°C)	20 °C

NOCT: Nominal operating-cell temperature.

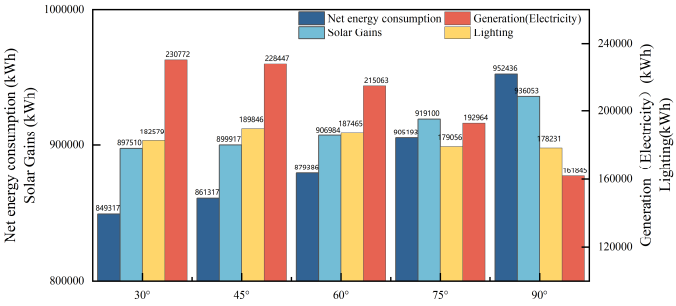
The connection method of the photovoltaic array on the building's external shading is also very important. The photovoltaic array is composed of multiple modules connected in series and parallel to meet the load's requirements. This configuration achieves the specified output current and voltage needed to supply power to the load, with the output power of the array being dependent on the number of modules connected. In this study, the photovoltaic panels used in the building have an operating voltage of approximately 40 V, and a battery system is utilized for energy storage and release (the battery's operating voltage is also 40 V, hence there is no need for parallel connection of the photovoltaic panels to increase voltage). Therefore, only parallel connection is employed to increase the current.

The key factor for external shading in buildings is the angle of the shading panels, as it directly affects the amount of solar radiation entering the interior and the power-generation efficiency of PV panels. To investigate this impact, five representative angles ranging from 30° to 90° were selected, specifically 30°, 45°, 60°, 75°, and 90°. The analysis was conducted using the energy simulation software DesignBuilder. The results are shown in Figure 14. For the building envelope facing east, the net energy consumption is the lowest when the angle

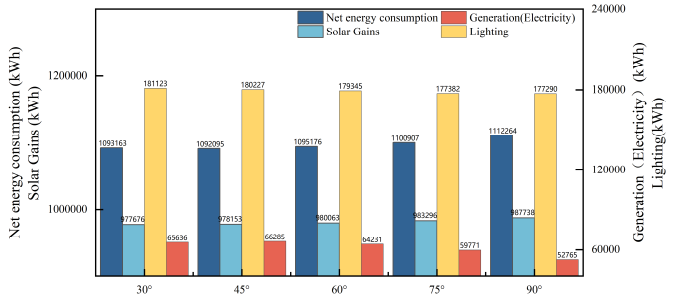
of the shading photovoltaic panel is 30°. This is mainly because as the angle of the shading photovoltaic panel increases, more outdoor sunlight enters the interior, reducing the indoor lighting's energy consumption by approximately 10,005 kWh. However, the increase in solar heat gain and the decrease in photovoltaic power generation lead to an increase in energy consumption of about 27,132 kWh, causing an overall upward trend in the building's energy consumption. Similarly, for the building envelope facing south, the net energy consumption is the lowest when the angle of the shading photovoltaic panel is 30°, as solar heat absorption and lighting energy consumption are minimized, while photovoltaic power generation is maximized. When the angle is increased to 90°, the indoor lighting's energy consumption is reduced by only 4348 kWh, but the overall building's energy consumption increases by approximately 123,853 kWh. For the building envelope facing west, the energy consumption is the lowest when the angle of the shading photovoltaic panel is 45°, and the net energy consumption is the highest when the photovoltaic shading panel angle is 90°.



(**a**) East orientation



(**b**) South orientation



(**c**) West orientation

Figure 14. Building energy consumption and PV panel power generation with shading in the east, south, and west orientations, respectively.

4.4. Optimization of Glass Structure Installation in the Library

Based on our research and survey, we proposed two retrofit solutions for the glass components of the building (Case 1 represents the building's energy consumption before any modifications). The first solution (Case 2) involves replacing the building's original low-E glass with photovoltaic (PV) glass. By leveraging the characteristics of STPV glass, we enhance the building's energy efficiency by adding power generation functionality without compromising light transmittance, thereby reducing the building's overall energy

consumption. The second solution (Case 3) aims to reduce indoor solar radiation by adding horizontal shading panels. Given that Changsha is located in a hot-summer and cold-winter region, solar heat-gain during summer (undesirable) far outweighs that in winter (beneficial). Photovoltaic panels are installed on top of these horizontal shading panels, providing both shading and electricity generation, which further reduces the building's energy demand. Both solutions also include modifications to the building's roof, where PV panels are installed. In Case 2, STPV glass directly replaces the original building glass, and the electricity generated is stored in batteries. When power is needed for the building's load, it is drawn directly from the battery storage. In Case 3, PV panels are mounted directly above the horizontal shading panels with an area of 2 m^2 (1 m × 2 m). There is a gap between the PV panels and the shading panels to allow air circulation, which helps mitigate the reduction in photovoltaic efficiency caused by temperature rise.

Based on Table 7, for Case 2, there is a positive optimization in zone heating and general lighting, while there is a negative optimization in total cooling and solar gain. Conversely, for Case 3, the situation is the opposite, with negative optimization in zone heating and general lighting and positive optimization in total cooling and solar gain. Looking at the annual energy consumption perspective, both Case 2 and Case 3 show reductions compared to Case 1. From the annual energy saving percentage perspective, Case 2 has a 7.42% annual energy saving percentage compared to Case 1, while Case 3 has a 12.6% annual energy saving percentage compared to Case 1. Therefore, overall, the optimization of Case 3 is superior to that of Case 2. Thus, for the renovation plan of the library, the use of sunshades along with PV panels and rooftop PV panels is preferable to photovoltaic glass and rooftop PV panels.

Table 7. Breakdown of annual energy consumption of the building for different retrofit scheme scenarios.

Programs	Refrigeration Energy Consumption	Heating Energy Consumption	Lighting Energy Consumption	Generation (Electricity)	Annual Energy Consumption	Annual Percent Energy Savings
	kWh	kWh	kWh	kWh	kWh	
Case 1	2,673,226	409,840	182,357	0	3,265,423	0
Case 2	3,009,805	349,022	162,593	−690,547	2,498,189	23.5%
Case 3	2,652,366	415,850	201,445	−1,152,120	2,035,069	35.4%

Based on the analysis in Figure 15 (Case 3), it can be understood that the months with the highest energy consumption are from May to September, which aligns with the fact that Changsha is located in southern China and has a subtropical monsoon climate. During the summer, daytime temperatures often exceed 30 °C, and at noon in July, temperatures can even reach above 35 °C, making July the month with the highest energy consumption throughout the year. Simultaneously, solar radiation in July is also the strongest, leading to the peak power generation capacity of the PV panels. In the figure, the energy coverage rates for April and November exceed 100%, indicating that the electricity generated by the PV panels during these months surpasses the building's total energy consumption. The energy coverage rates for February, March, May, October, and December exceed 40%, demonstrating that the PV panels effectively reduce the building's total energy consumption during these months as well. Only July and August have relatively low energy coverage rates, at 17.85% and 18.18%, respectively. This may be due to the high temperatures during these two summer months, leading to increased energy consumption by the building's air conditioning system. Although the power-generation capacity of the PV panels is high, it cannot completely cover the energy demand during these high-consumption periods.

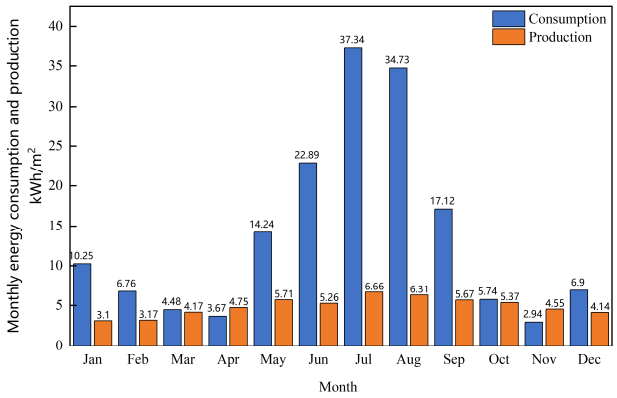
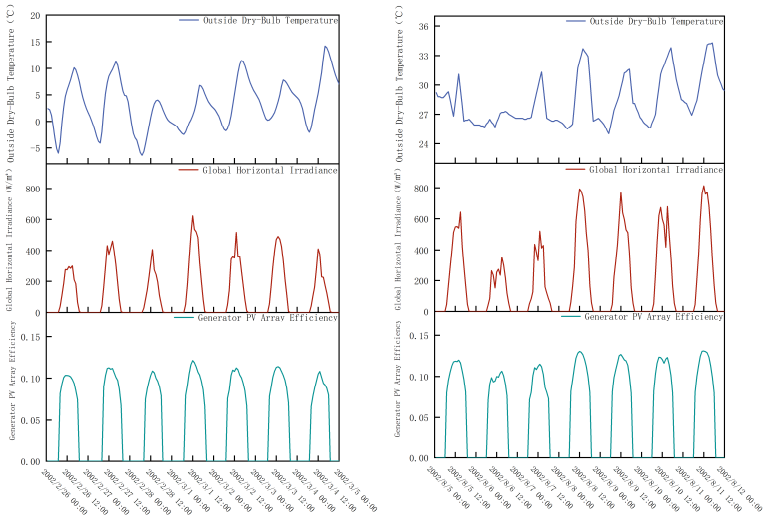


Figure 15. Monthly building energy consumption and PV panel energy production comparison.

4.5. Evaluation of PV Array Efficency for Summer and Winter Typical Weeks

Figure 16 shows the variations in outdoor dry-bulb temperature, global horizontal irradiance, and photovoltaic (PV) array conversion efficiency during a typical week in summer and winter in Changsha. A comparison reveals significant differences in the performance of the PV system under different seasonal conditions. Our goal is to use the typical weekly meteorological data to evaluate and predict the conversion efficiency of PV panels under different climatic conditions.



(**a**) a typical week in winter (**b**) a typical week in summer

Figure 16. Simulated results of power generation by PV array for a typical week in summer and winter.

In summer, the outdoor dry-bulb temperature remains relatively high, with an average temperature between 27 °C and 36 °C, and the peak global horizontal irradiance reaches around 800 W/m^2. Although high temperatures may have a certain impact on the efficiency of the PV array, due to the higher irradiance intensity, the conversion efficiency of the PV array remains in the higher range, between 0.10 and 0.12

In contrast, during winter, the outdoor dry-bulb temperature is lower, ranging from approximately 0 °C to 15 °C, and the peak global horizontal irradiance is also relatively lower, reaching only about 600 W/m^2. Although the decrease in temperature is more favorable for the operating temperature of the PV array, the reduced solar irradiance results in the conversion efficiency of the PV array remaining within the range of 0.10 to 0.13. Similar to summer, there are noticeable fluctuations in efficiency during daytime hours.

Overall, the conversion efficiency of the PV array remains relatively stable between 0.1 and 0.13 across different seasons.

5. Payback Period

The simulation conducted using DesignBuilder software indicates that the total area required for photovoltaic panels for building retrofitting is 3594 square meters. The market price of these photovoltaic panels is 1.5 yuan per watt, which translates to 337.5 yuan per square meter, including installation costs. The initial investment for the photovoltaic panels amounts to 1,212,975 yuan. In Changsha, a peak–valley electricity pricing system is in place, with peak hours from 7:00 to 11:00 and 17:00 to 21:00 daily, at a peak rate of 0.588 yuan per kilowatt-hour. Off-peak hours are from 11:00 to 17:00 and 21:00 to 23:00, with an off-peak rate of 0.538 yuan per kilowatt-hour. On average, the electricity price is calculated at 0.563 yuan per kilowatt-hour. This photovoltaic system is estimated to generate approximately 1,151,120 kilowatt-hours of electricity annually, resulting in savings of about 648,643 yuan per year. The payback period for this investment is 1.87 years.

6. Conclusions

This study thoroughly analyzed the energy consumption of a library in Changsha and proposed two energy-saving solutions by integrating BIPV technology into the building's renovation. Using DesignBuilder software for simulation, this study reached the following conclusions:

1. Although the target building for renovation in this study is a library located in the Changsha region, and the results are specifically applicable to buildings in that area, the primary objective of this paper is to explore and disseminate the renovation concept. This method can be applied to the renovation of public buildings in regions with hot summers and cold winters. In these areas, the solar heat-gain in summer (unfavorable) is much greater than in winter (favorable). Therefore, by skillfully using horizontal sunshades and installing photovoltaic panels above them, it is possible to reduce the building's solar heat-gain while enhancing power generation, thereby lowering the building's energy consumption. The experimental validation of the simulation results has proven the reliability of the simulation method. This provides a solid data foundation for further optimization, ensuring that the simulation results are of high value.
2. Although the target building for renovation in this study is a library located in the Changsha region, and the renovation results are only applicable to buildings in that area, the main objective of this paper is to develop a renovation plan for public buildings in other regions with hot summers and cold winters based on the study of this library. In such regions, the solar heat-gain during summer (unfavorable) is significantly greater than during winter (favorable). Therefore, by skillfully using horizontal sunshades and installing photovoltaic panels above them, it is possible to reduce the building's solar heat-gain while enhancing power generation, ultimately reducing energy consumption.
3. The first solution involves installing PV panels on the roof and photovoltaic sunshades on the windows, reducing annual energy consumption by 35.4%. The second solution involves installing PV panels on the roof and photovoltaic glass, reducing annual energy consumption by 23.5%. These solutions not only enhance rooftop photovoltaic power generation but also achieve more efficient building-integrated power generation through shading facilities and photovoltaic glass, optimizing indoor lighting and temperature regulation.
4. The comprehensive renovation combining PVs, BIPVs, and external shading technologies significantly improves the building's energy efficiency, demonstrating the great potential of multi-technology coupling in building energy conservation. As demonstrated in Section 6, although the initial investment is high, the long-term energy cost-savings and environmental benefits are substantial, offering good economic returns. Additionally, reducing the building's reliance on traditional fossil fuels effectively lowers carbon emissions, contributing to the achievement of carbon peak and carbon neutrality goals.

Future research should further optimize the design and layout of photovoltaic systems, particularly the combined application of sunshades and photovoltaic glass, to explore more efficient power-generation methods. It is also recommended to introduce intelligent photovoltaic control systems and energy management systems to enhance the system's intelligence and automation levels.

This study proposes an efficient energy-saving solution through the integration of photovoltaic technology into the renovation of a library building located in Changsha, significantly reducing the building's energy consumption. The results not only provide valuable reference for energy-saving renovations in this region but also offer a feasible technical approach for public buildings in similar climate conditions globally. From the perspective of sustainable development, Building-Integrated Photovoltaic (BIPV) technology harnesses solar energy, a clean and renewable resource, to reduce reliance on fossil fuels and lower carbon emissions. This contributes not only to addressing climate change but also to promoting the transition of the energy structure towards decarbonization and renewable sources.

Author Contributions: Conceptualization, Z.D.; methodology, Z.D.; writing—original draft preparation, G.X. and K.S.; supervision and funding acquisition, Z.D.; writing—review and editing, Z.D., G.X. and X.D.; analysis and validation, G.X.; visualization, G.X. All authors have read and agreed to the published version of the manuscript.

Funding: This research was funded by the Beijing Natural Science Foundation (Grant No. 3222028), the Pyramid Talent Training Project of Beijing University of Civil Engineering and Architecture (Grant No. JDYC20200314), the National Natural Science Foundation of China (Grant No. 51908020), and the BUCEA Post Graduate Innovation Project (No. PG2024060).

Data Availability Statement: The data presented in this study are available on request from the corresponding author.

Conflicts of Interest: The authors declare no conflicts of interest.

Abbreviations

The following abbreviations, variables and subscripts are used in this manuscript:

α	The remainder of the sun's altitude Angle,°
β	PV panels tilt angle,°
θ	Local latitude
θ_{az}	Solar azimuth angle,°
Θ_{elev}	Solar altitude angle,°
PV	Photovoltaic
BIPV	Building-Integrated Photovoltaics
NWP	Numerical weather prediction
ANNs	Artificial neural networks
GISs	Geographic Information Systems
SHGC	Solar Heat Gain Coefficient
$S_{incident}$	The amount of direct radiation received by the photovoltaic panel, W/m^2
S_{module}	The vertical component of the direct radiation, W/m^2
$S_{module.h}$	The horizontal component of the direct radiation, W/m^2
$S_{diffuse}$	The amount of diffuse radiation, W/m^2
$S_{horizontal}$	The vertical component of the solar radiation to the ground, W/m^2
VT	Visible Transmittance
TPP	Total radiation received on the surface of the photovoltaic panel, W/m^2

References

1. Mekhilef, S.; Saidur, R.; Safari, A.; Mustaffa, W.E.S.B. Biomass energy in Malaysia: Current state and prospects. *Renew. Sustain. Energy Rev.* **2011**, *15*, 3360–3370. [CrossRef]
2. Tan, Z.; Zhang, H.; Xu, J.; Wang, J.; Yu, C.; Zhang, J. Photovoltaic Power Generation in China: Development Potential, Benefits of Energy Conservation and Emission Reduction. *J. Energy Eng.* **2012**, *138*, 73–86. [CrossRef]

3. Rosas-Flores, J.A.; Zenón-Olvera, E.; Gálvez, D.M. Potential energy saving in urban and rural households of Mexico with solar photovoltaic systems using geographical information system. *Renew. Sustain. Energy Rev.* **2019**, 116. [CrossRef]
4. Ishii, S.; Tabushi, S.; Aramaki, T.; Hanaki, K. Impact of future urban form on the potential to reduce greenhouse gas emissions from residential, commercial and public buildings in Utsunomiya, Japan. *Energy Policy* **2010**, *38*, 4888–4896. [CrossRef]
5. Silvestre, S.; Tahri, A.; Tahri, F.; Benlebna, S.; Chouder, A. Evaluation of the performance and degradation of crystalline silicon-based photovoltaic modules in the Saharan environment. *Energy* **2018**, *152*, 57–63. [CrossRef]
6. Cludius, J.; Hermann, H.; Matthes, F.C.; Graichen, V. The merit order effect of wind and photovoltaic electricity generation in Germany 2008–2016: Estimation and distributional implications. *Energy Econ.* **2014**, *44*, 302–313. [CrossRef]
7. Kaplanis, S.; Kaplani, E. A new dynamic model to predict transient and steady state PV temperatures taking into account the environmental conditions. *Energies* **2018**, *12*, 2. [CrossRef]
8. Gulin, M.; Pavlović, T.; Vašak, M. Photovoltaic panel and array static models for power production prediction: Integration of manufacturers' and on-line data. *Renew. Energy* **2016**, *97*, 399–413. [CrossRef]
9. Tanaka, K.; Uchida, K.; Ogimi, K.; Goya, T.; Yona, A.; Senjyu, T.; Funabashi, T.; Kim, C.-H. Optimal Operation by Controllable Loads Based on Smart Grid Topology Considering Insolation Forecasted Error. *IEEE Trans. Smart Grid* **2011**, *2*, 438–444. [CrossRef]
10. Zhang, P.; Takano, H.; Murata, J. Daily solar radiation prediction based on wavelet analysis. In Proceedings of the IEEE SICE Annual Conference, Tokyo, Japan, 13–18 September 2011; pp. 712–717.
11. Wang, F.; Mi, Z.; Su, S.; Zhao, H. Short-Term Solar Irradiance Forecasting Model Based on Artificial Neural Network Using Statistical Feature Parameters. *Energies* **2012**, *5*, 1355–1370. [CrossRef]
12. Enkvist, P.-A.; Dinkel, J.; Lin, C. *Impact of the financial Crisis on Carbon Economics: Version 2.1 of the Global Greenhouse Gas Abatement Cost Curve*; McKinsey & Company: New York, NY, USA, 2010; p. 374.
13. Huide, F.; Xuxin, Z.; Lei, M.; Tao, Z.; Qixing, W.; Hongyuan, S. A comparative study on three types of solar utilization technologies for buildings: Photovoltaic, solar thermal and hybrid photovoltaic/thermal systems. *Energy Convers. Manag.* **2017**, *140*, 1–13. [CrossRef]
14. Johnson, R.; Sullivan, R.; Selkowitz, S.; Nozaki, S.; Conner, C.; Arasteh, D. Glazing energy performance and design optimization with daylighting. *Energy Build.* **1984**, *6*, 305–317. [CrossRef]
15. Lee, J.W.; Jung, H.J.; Park, J.Y.; Lee, J.B.; Yoon, Y. Optimization of building window system in Asian regions by analyzing solar heat gain and daylighting elements. *Renew. Energy* **2013**, *50*, 522–531. [CrossRef]
16. Wilson, R.; Young, A. The embodied energy payback period of photovoltaic installations applied to buildings in the UK. *Build. Environ.* **1996**, *31*, 299–305. [CrossRef]
17. Alsadi, S.Y.; Nassar, Y.F. Estimation of Solar Irradiance on Solar Fields: An Analytical Approach and Experimental Results. *IEEE Trans. Sustain. Energy* **2017**, *8*, 1601–1608. [CrossRef]
18. Sidek, M.H.M.; Azis, N.; Hasan, W.Z.W.; Ab Kadir, M.Z.A.; Shafie, S.; Radzi, M.A.M. Automated positioning dual-axis solar tracking system with precision elevation and azimuth angle control. *Energy* **2017**, *124*, 160–170. [CrossRef]
19. Mahmoud, Y.; El-Saadany, E.F. A Novel MPPT Technique Based on an Image of PV Modules. *IEEE Trans. Energy Convers.* **2017**, *32*, 213–221. [CrossRef]
20. Hartner, M.; Ortner, A.; Hiesl, A.; Haas, R. East to west—The optimal tilt angle and orientation of photovoltaic panels from an electricity system perspective. *Appl. Energy* **2015**, *160*, 94–107. [CrossRef]
21. Siraki, A.G.; Pillay, P. Study of optimum tilt angles for solar panels in different latitudes for urban applications. *Sol. Energy* **2012**, *86*, 1920–1928. [CrossRef]
22. Benghanem, M. Optimization of tilt angle for solar panel: Case study for Madinah, Saudi Arabia. *Appl. Energy* **2011**, *88*, 1427–1433. [CrossRef]
23. Dhimish, M.; Silvestre, S. Estimating the impact of azimuth-angle variations on photovoltaic annual energy production. *Clean Energy* **2019**, *3*, 47–58. [CrossRef]
24. He, W.; Zhang, Y.; Sun, W.; Hou, J.; Jiang, Q.; Ji, J. Experimental and numerical investigation on the performance of amorphous silicon photovoltaics window in East China. *Build. Environ.* **2011**, *46*, 363–369. [CrossRef]
25. Young, C.-H.; Chen, Y.-L.; Chen, P.-C. Heat insulation solar glass and application on energy efficiency buildings. *Energy Build.* **2014**, *78*, 66–78. [CrossRef]
26. Singh, R.; Banerjee, R. Estimation of roof-top photovoltaic potential using satellite imagery and GIS. In Proceedings of the 2013 IEEE 39th Photovoltaic Specialists Conference (PVSC), Tampa, FL, USA, 16–21 June 2013; pp. 2343–2347.
27. Zhong, Q.; Tong, D. Spatial layout optimization for solar photovoltaic (PV) panel installation. *Renew. Energy* **2020**, *150*, 1–11. [CrossRef]
28. Mesloub, A.; Albaqawy, G.A.; Kandar, M.Z. The Optimum Performance of Building Integrated Photovoltaic (BIPV) Windows Under a Semi-Arid Climate in Algerian Office Buildings. *Sustainability* **2020**, *12*, 1654. [CrossRef]
29. Abdelhakim, M.; Kandar, M.Z.; Lim, Y.W. Experimental Investigation of Overall Energy Performance in Algerian Office Building Integrated Photovoltaic Window under Semi-Arid Climate. *J. Daylighting* **2019**, *6*, 23–41. [CrossRef]
30. Fung, T.Y.Y.; Yang, H. Study on thermal performance of semi-transparent building-integrated photovoltaic glazings. *Energy Build.* **2008**, *40*, 341–350. [CrossRef]

31. Mesloub, A.; Ghosh, A.; Touahmia, M.; Albaqawy, G.A.; Noaime, E.; Alsolami, B.M. Performance Analysis of Photovoltaic Integrated Shading Devices (PVSDs) and Semi-Transparent Photovoltaic (STPV) Devices Retrofitted to a Prototype Office Building in a Hot Desert Climate. *Sustainability* **2020**, *12*, 10145. [CrossRef]
32. Mesloub, A.; Ghosh, A. Daylighting Performance of Light Shelf Photovoltaics (LSPV) for Office Buildings in Hot Desert-Like Regions. *Appl. Sci.* **2020**, *10*, 7959. [CrossRef]
33. Mesloub, A.; Ghosh, A.; Albaqawy, G.A.; Noaime, E.; Alsolami, B.M. Energy and Daylighting Evaluation of Integrated Semi-transparent Photovoltaic Windows with Internal Light Shelves in Open-Office Buildings. *Adv. Civ. Eng.* **2020**, *2020*, 8867558. [CrossRef]
34. Yoon, J.-H.; Song, J.; Lee, S.-J. Practical application of building integrated photovoltaic (BIPV) system using transparent amorphous silicon thin-film PV module. *Sol. Energy* **2011**, *85*, 723–733. [CrossRef]
35. Cronemberger, J.; Corpas, M.A.; Cerón, I.; Caamaño-Martín, E.; Sánchez, S.V. BIPV technology application: Highlighting advances, tendencies and solutions through Solar Decathlon Europe houses. *Energy Build.* **2014**, *83*, 44–56. [CrossRef]

Disclaimer/Publisher's Note: The statements, opinions and data contained in all publications are solely those of the individual author(s) and contributor(s) and not of MDPI and/or the editor(s). MDPI and/or the editor(s) disclaim responsibility for any injury to people or property resulting from any ideas, methods, instructions or products referred to in the content.